

## A Comparative Study of NiZn Ferrites Modified by the Addition of Cobalt

S.L. Pereira<sup>a</sup>, H.-D. Pfannes<sup>a</sup>, A.A. Mendes Filho<sup>b</sup>,

L.C.B. de Miranda Pinto<sup>b</sup>, M.A. Chincaro<sup>c</sup>

<sup>a</sup>Departamento de Física da Universidade Federal de Minas Gerais,  
Av. Antônio Carlos 6627, 30123-970 Belo Horizonte - MG, Brazil

<sup>b</sup>Setor de Materiais Ópticos e Eletrônicos da Fundação Centro Tecnológico de Minas Gerais  
Av. José Cândido da Silveira 2000, 31170-000 Belo Horizonte - MG, Brazil

<sup>c</sup>Setor de Testes Físicos da Fundação Centro Tecnológico de Minas Gerais  
Av. José Cândido da Silveira 2000, 31170-000 Belo Horizonte - MG, Brazil

Received: August 15, 1998; Revised: March 30, 1999

Off-stoichiometric NiZn ferrite was obtained by hydrothermal process and compacted in torus form under different pressures. Two samples A1 and A2 - cobalt doped (0.5 %) were sintered at 1573 K in air atmosphere during 3 h. The magnetic properties were studied by vibrating sample magnetometry, Mössbauer spectroscopy and complex impedanciometry. X-ray diffraction and Hg porosimetry were used in order to determine the average grain size and the type of packing in the samples. Both samples exhibited superparamagnetic behavior in the hysteresis loop. This effect does not agree with Mössbauer results, which were fitted using Normos, a commercial computer program. All samples parameters were compared.

**Keywords:** NiZn ferrites

### 1. Introduction

Stoichiometric nickel-zinc ferrite ( $x = 0.65$ ), described by the formula  $\text{Ni}_x\text{Zn}_{1-x}\text{Fe}_2\text{O}_4$ , has been of interest due to technological applications in high frequency inductors, transformer cores, microwave devices, etc. Magnetic properties are determined by chemical composition, porosity, grain size and microstructure.

Nickel-zinc ferrite has spinel structure. There are eight tetrahedral sites occupied by non-magnetic  $\text{Zn}^{2+}$  ions and sixteen octahedral sites occupied by  $\text{Ni}^{2+}$  and  $\text{Fe}^{3+}$  ions. Due to the synthesis process or off-stoichiometry, some iron on octahedral sites may be in the divalent state ( $\text{Fe}^{2+}$ ) and affects the magnetic and electric properties. Cobalt has been introduced in the chemical composition (less than 1%), in order to improve magnetic properties<sup>1</sup>. This ion creates a crystal-field stabilized by a Jahn-Teller<sup>2,3</sup> effect and spin orbit in an octahedral site. Its main effect on the Mössbauer spectrum is a distortion of the octahedral site.

In off-stoichiometric formula, like the samples used in this study, octahedral site  $\text{Fe}^{2+}$  ions are present (often in the form of  $\text{Fe}_3\text{O}_4$  or  $\text{Fe}_2\text{O}_3$ ). These ions may combine with

impurities (carbon) to create a non-magnetic layer around the ferrite grains and propitiate the appearance of other phases in the Mössbauer spectrum.

In this study, samples were prepared under similar conditions (*i.e.* porosity, sinterization and autoclave synthesis time) to allow for a comparison of the effects of cobalt addition on the magnetic properties and hyperfine parameters.

### 2. Experimental

NiZn ferrite ( $\text{Ni}_x\text{Zn}_{1-x}\text{Fe}_2\text{O}_4$ , nominal composition  $x = 0.5$ ) was synthesized by hydrothermal process in an autoclave at 408 K during 20 h. An amount of 0.5 % of cobalt was added as impurity in one sample and both samples were pressed employing PVA (polyvinyl alcohol) as powder binder. Two samples, labeled A1 and A2 (doped) were obtained in a torus form by application of pressure of 122.8 MPa. The ceramic bodies were sintered at 1573 K during 3 h in air atmosphere. The porosity of the samples was determined using Hg porosimetry in a model 4220 Autopore II porosimeter manufactured by Micromeritics.

A Rigaku Geigerflex powder diffractometer operating with CuK and having a graphite crystal monochromator ([0002],  $2d = 6,708 \text{ \AA}$ ) between sample and detector was used in order to determine the average crystallite sizes from the X-ray diffraction line broadening measurements by using the Scherrer formula<sup>4</sup>,

$$d_0 = \frac{0.94 \lambda}{\beta (2\theta) \cos\theta}$$

where

$\lambda$  is the X-ray wavelength;

$\beta (2\theta)$  is the width at half height; and

$\theta$  is the diffraction angle.

The magnetic permeability was measured using an impedance analyzer (HP 4192A) with a winding of 30 turns around the torus and frequency range 10 - 13 MHz. For the DC magnetometry, both samples were prepared by grinding. 21 mg of the resulting powder were inserted in a cylindrical sample holder for measurements in a model 4500 VSM manufactured by EGG& Janis. The Mössbauer spectra were obtained using an acceleration constant spectrometer and  $\text{Co}^{57}/\text{Rh}$  source.

### 3. Results and Discussion

Figure 1 presents part of the X-ray diffraction pattern (311 peaks - relative to Si - standard) of the ferrites. These patterns exhibit small differences due to average grain size and lattice constant ( $d_0 = 41.6 \text{ nm}$ ,  $a = 8.395 \pm 0.005 \text{ \AA}$  for sample A1 and  $d_0 = 39.7 \text{ nm}$ ,  $8.384 \pm 0.005 \text{ \AA}$  for sample A2). Due to cobalt addition, the lattice constant presents a very small shrinkage and peaks (311) exhibit but a small shift toward large angles between samples. Table 1 shows the main results of porosimetry and impedanciometry. The porosity values indicate that the ceramic body has dense random packing<sup>5</sup>.

The saturation magnetization  $M_s$  was obtained by extrapolating  $M(1/H)$ -curves to  $1/H = 0$ . Its values are (24.9 emu/g for A1 and 41.6 emu/g for A2) comparable to

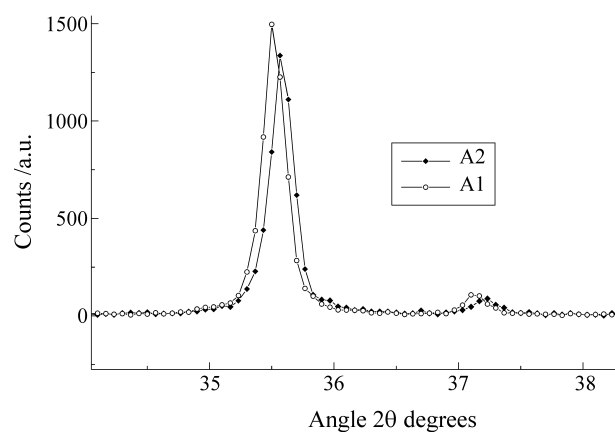


**Figure 1.** A small X-ray shift between samples A1 and A2 (doped).

reference<sup>6</sup>, which presented a similar study in which samples were prepared using the aerosol technique. In Fig. 2 the hysteresis for both samples exhibit narrow loops. This may imply that samples are superparamagnetic, in the time window of the VSM. Despite the fact that lattice constant and average grain size be so close, the magnetization in sample A1 is lower than in A2. It is reasonable to assume that other phases, such as hematite and carbon, may act as non-magnetic layers, thus diminishing the magnetization<sup>7-9</sup> of the samples.

The theory described by Johnson *et al.*<sup>8,9</sup> for permeability was used to calculate the average size of the non-magnetic shell around the ferrite grains, as per the following equation:

**Table 1.** Density, porosity and relative permeability of the samples A1 and A2.

Sample	Green density [kgm <sup>-3</sup> ]	Final density [kgm <sup>-3</sup> ]	Porosity [cm <sup>3</sup> ] of Hg	Permeability At 1 kHz
A1	3.03	4.90	0.62	480
A2	2.43	4.10	0.66	546

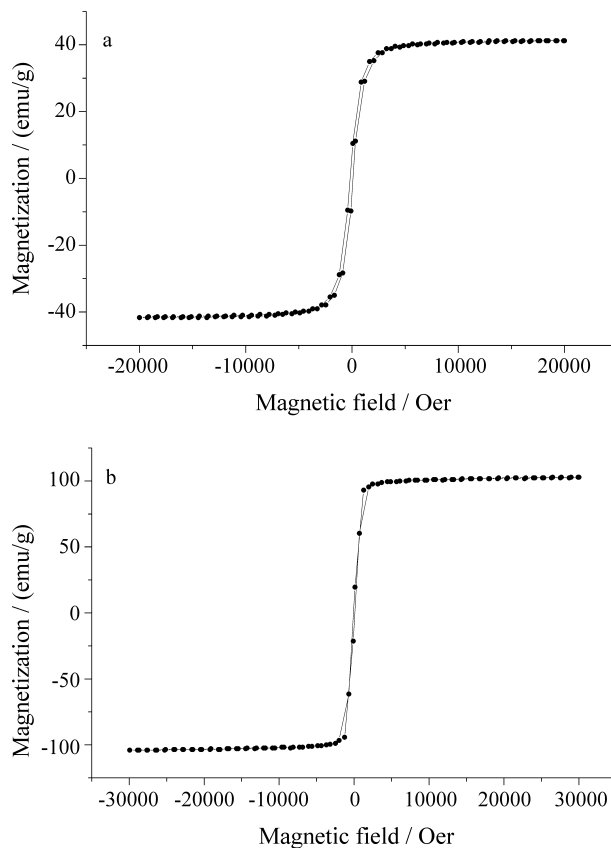


**Figure 2.** Very thin hysteresis loops: a) sample A2 - exhibits roundness knee and b) sample A1 - shows several crossings that indicates other phases present.

$$\mu_e = \frac{\mu_i D_0}{\mu_i \delta + D_0}$$

where

$\mu_e$  is the rotational permeability;

$\mu_i$  is initial permeability; and

$D_0$  is the average grain size.

Values of  $\mu_e$  were extrapolated from the M(H)-curves at low field values (19.77 for A1 and 24.0 for A2). The initial permeability was taken from Table 1 and  $D_0$  was calculated according to (1). The non-magnetic layers (2.02 nm for A1 and 1.58 nm for A2) are too thin to significantly contribute to the hysteresis loop.

The Mössbauer spectra (Fig. 3) exhibits A and B sites whose parameters differ between samples. The addition of cobalt does not affect the tetrahedral sites and affected only very little the B-sites. In other words, the hyperfine field on the octahedral sites seems not to have changed. The charge density of the  $\text{Fe}^{2+}$  ions in the octahedral site diminished (see Table 1 - isomer shift ( $\delta$ )). The octahedral distortion in the sample A2 is small ( $\Delta$  (A1) <  $\Delta$  (A2)). There are two other components in the spectra, a doublet and a sextet in the interstitial site. The sextet of the interstitial site has its charge density diminished and its hyperfine field too. In the doublet the charge density increases as well as the quadrupole splitting. We could identify that the doublet is characteristic of the  $\text{Fe}^{2+}$  as it is in iron oxide samples.  $\text{FeCO}_3$  may be also present, according to the parameters and the asymmetry between its lines<sup>10</sup>. The amount of binder was not controlled, thus making it difficult to evaluate how much

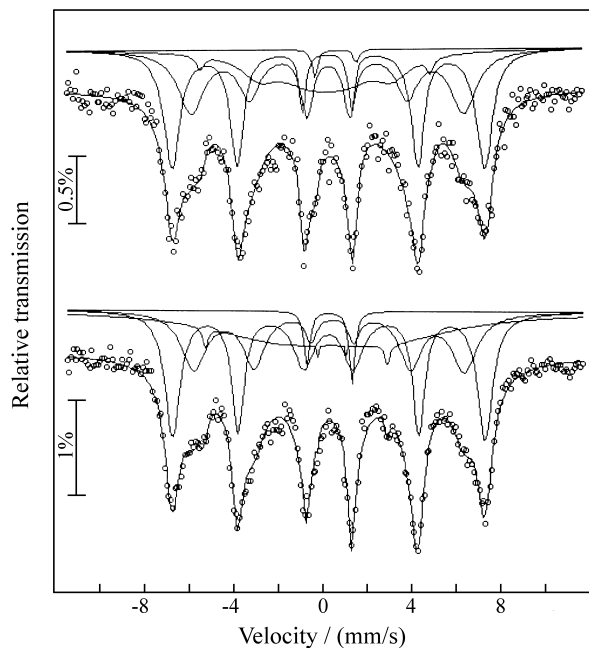


**Figure 3.** Mössbauer spectra of the samples at 300 K - A1 (up) and A2 (down).

**Table 2.** Mössbauer parameters of the samples.

Sample	Site	$\delta^*$ (mm/s)	$\Delta$ (mm/s)	BHF (T)	Area (%)
A1	A	0.17 (1)	0.04 (2)	43.6 (1)	39.5
	B	0.18 (2)	-0.04 (4)	38.0 (5)	35.2
		-0.16 (6)	-0.5 (1)	32.1 (4)	24
		0.54 (5)	1.87 (9)	-	1.23
A2	A	0.17 (0)	0.02 (1)	43.6 (3)	39.74
	B	0.27 (2)	-0.14(3)	37.7 (1)	26.12
		-0.47 (4)	-0.59 (7)	25.4 (3)	30.77
		0.21 (1)	2.03 (2)	-	3.21

\* relative to  $\alpha$ -iron.

( ) uncertainty values.

carbon participates in the interstitial site. The parameters in Table 2 show that samples are not superparamagnetic. The in-homogeneity in these samples seems to be the main cause of the spin relaxation<sup>11</sup>.

#### 4. Conclusion

It was observed that cobalt addition in amounts less than 1% improves the magnetic characteristics of the ferrites. When cobalt ion penetrates in the octahedral site, it replaces iron ion that goes to interstitial site and may combine with carbon. If sintering temperature is high enough other phases may appear in the ceramic body.

The method used to evaluate the average size of the non-magnetic layer need to reproduce the magnetization curve to be acceptable. *A posteriori* good approximation could be obtained using this method and a Langevin function weighted with Log-normal distribution.

Although superparamagnetism was expected, the Mössbauer spectra exhibited spin relaxation, possibly due to the crystallite size to be less than the average size evaluated by X-ray diffraction. The non-magnetic layer presented itself much too thin to affect hysteresis loop and imposes a superparamagnetic characteristic.

#### Acknowledgments

The authors gratefully acknowledge the support of CAPES, CNPq and FAPEMIG.

#### References

1. Tebble, R.S.; Craik, D.J. *Magnetic Materials*, Wiley-Interscience, London, p. 619, 1969.
2. Abragam, A.; Bleaney, B. *Electron Paramagnetic Resonance of Transition Ions*, Dover Publications, Inc., NY, Ch. XXI, p. 790, 1986.
3. Craik, D. *Magnetism - Principles and Applications*, John-Wiley & Sons, Chichester, England, p. 99, 203 and followings, 1995.

4. Warren, B.E. *X-ray Diffraction*, Addison-Wesley, Reading, MA, p. 253, 1980.
5. *Disorder and Granular Media*, Bideau, D.; Hansen, A., eds., Elsevier Science Publishers B. V. , Amsterdam, 1993.
6. de Marco, M.; Wang, X.W.; Snyder, R.L.; Simmins, J.; Bayya, S.; White, M.; Naughton, M.J. *J. Appl. Phys.*, v. 73, n. 10, 1993.
7. Nakamura, T.; Tsutaoka, T.; Hatakeyama, K. *J. Magn. Magn. Mater.*, n. 138, p. 319-28, 1994.
8. Johnson, M.T.; Visser, E.G. *IEEE Trans. Magn.*, v. 26, n. 5, p. 1987-89, 1990.
9. Johnson, M.T.; Noordermeer, A.; Severin, M.M.E.; Meeuwissen, W.A.M. *J. Magn. Magn. Mater.*, n. 116, p. 169-176, 1992.
10. Greenwood, N.N.; Gibb, T.C. *Mössbauer Spectroscopy*, Chapman and Hall Ltd., London, 1971.
11. Ling, Qi-Fen; Li, Guo-Dong; Li, De-Xin; Guo, Shu-Jiao. *J. Appl. Phys.*, v. 73, n. 10, p. 6290-91, 1993.